

Article

Magnesium/Silica/Lanthanum@Activated Carbon for the Remediation of As(III) from Water

Athanasia K. Tolkou  and George Z. Kyzas 

Hephaestus Laboratory, Department of Chemistry, International Hellenic University, GR-65404 Kavala, Greece; kyzas@chem.ihu.gr

* Correspondence: tolkatha@chem.ihu.gr; Tel.: +30-2510-462-218

Abstract: In this study, activated carbon was suitably modified with Mg/Si/La and its effectiveness in removing As(III) was investigated. The structure of Magnesium/Silica/Lanthanum@Activated Carbon (Mg-Si-La@AC) was fully characterized and several parameters, such as the dosage, pH, contact time, and initial As(III) concentration, were studied. Thus, the BET surface area, total pore volume, and micropore volume of Mg-Si-La@AC were measured to be 271.46 m²/g, 0.006 cm³/g and 0.52 cm³/g, respectively. The results showed that the optimal condition for the reduction in As(III) from the initial concentration of 100 µg/L to below 10 µg/L was the addition of 1.5 g/L of adsorbent at pH 7.0. Furthermore, 4 h of contact time showed >90% removal. The Langmuir isotherm model was best fitted to the experimental results, exhibiting a maximum adsorption capacity of 322 µg/g, and the PSO kinetic model was found to be the most applicable according to kinetics. Consecutive regeneration studies were carried out and the results showed that the adsorbent was effectively used up to four cycles.

Keywords: arsenic; adsorption; activated carbon; magnesium; lanthanum; silicate



Citation: Tolkou, A.K.; Kyzas, G.Z. Magnesium/Silica/Lanthanum@Activated Carbon for the Remediation of As(III) from Water. *Environments* **2023**, *10*, 171. <https://doi.org/10.3390/environments10100171>

Academic Editor: Simeone Chianese

Received: 10 September 2023

Revised: 28 September 2023

Accepted: 29 September 2023

Published: 3 October 2023



Copyright: © 2023 by the authors. Licensee MDPI, Basel, Switzerland. This article is an open access article distributed under the terms and conditions of the Creative Commons Attribution (CC BY) license (<https://creativecommons.org/licenses/by/4.0/>).

1. Introduction

Groundwater contamination is a major global environmental concern [1], with many social implications, and can be caused by both human activities and nature. Millions of people in numerous countries, including Bangladesh, Pakistan, Vietnam, Cambodia, India, Argentina, Chile, etc. [2–5], are at risk of high As levels via groundwater consumption. In Pakistan, As was also found, in addition to groundwater [6], in land uses, with dust levels being highest in industrial areas [7]. Arsenic occurs in water as well as in air and soil [1], but it is very toxic in its inorganic form, found as tri-valent (arsenite) or pentavalent (arsenate), especially in its +3 oxidation state (As(III)) [8]. Long-term exposure to arsenic can cause chronic arsenic poisoning, with skin lesions and skin cancer being the most typical consequences [9,10]. In addition, liver or lung cancer, along with a variety of other effects, can also be caused by consuming arsenic via drinking water or food [11]. Consequently, the World Health Organization (WHO) has defined 10 µg/L as the suggested limit for arsenic in drinking water [12]. To maintain the WHO limits, new more effective elimination techniques should be applied, or existing ones should be modified and optimized accordingly. Numerous removal techniques [13] have been established for arsenic elimination from water, such as coagulation [14], adsorption [15], membranes [16,17], precipitation [18,19], ion exchange [20], etc. Comparing these methods, it appears that chemical precipitation and coagulation–flocculation are widely used due to their simplicity. The membrane filtration process is also effective; however, its operating cost is very high and due to membrane fouling, it is disadvantageous. The ion exchange method is a method in which anions and cations are exchanged in solution, but it fails in concentrated metal solutions. These processes are pH-dependent and therefore require the constant monitoring and control of pH. Consequently, the aforementioned procedures have some drawbacks, such as the high cost of both operation and construction, offer the

partial removal of certain ions and contribute to high sludge production, thus increasing the operating cost for sludge disposal [21,22]. Adsorption, widely used to remove dyes from aqueous solutions [23–25], is possibly one of the most popular methods for heavy metal and oxyanion elimination, and includes the application of a material that removes the pollutant from the water by binding ions to its surface. A wide range of adsorbents, natural or modified, have been tested successfully for arsenic removal. Among them, there are various minerals such as zeolite [26], silica [27], goethite [28], and calcite [29,30], and also activated carbons [14,31,32], biosorbents [33,34], biochars [35], graphene oxides [36], polyethylenimine-modified materials [37], and metal–organic frameworks (MOFs) [38], etc. In addition, synthetic adsorbents such as CeO₂–ZrO₂ nanospheres [39], molecularly imprinted polymers [40], and the combination of Fe(III)-H₂O₂ [41] and Fe-Mn binary oxides [42], or the addition of graphene oxide/granular ferric hydroxide (GO/GFH) [36], have also been applied in arsenic removal studies.

Among these adsorbents, activated carbon (AC) has been generally used to remove heavy metals from water. A plethora of materials have been produced in several studies by using low-cost origin materials, such as coconut and palm shell, potatoes, fruit peels, bamboo, canola stalks [43–46], etc., as the interest of researchers is high for lower-cost activated carbon sources. Recently, the impregnation of activated carbons with various additives has been widely studied, with the aim of increasing their surface area to make them more suitable for heavy metal and oxyanion removal. The modification of activated carbon offers the chemical groups dispersed within it, resulting in both the optimization of the prevailing activated carbon properties and the enhanced synergy between these chemical groups and the carbon, with the aim of enhancing the removal of various substances (e.g., dyes, heavy metals, etc.) [47,48]. Charged metal cations, which contain high positive charges, can probably recruit several oxyanions such as arsenic. Therefore, several rare earth elements, among them lanthanum, have been used for arsenic removal and exhibited a relative affinity [49]. Consequently, AC has been lately modified with cerium dioxide (PAC–CeO₂), which is a nontoxic rare earth oxide, and found to be highly effective as an adsorbent for the elimination of arsenic from drinking water [50]. Similar studies have combined lanthanum and cerium functionalities to modify activated carbon prepared from avocado kernel seeds [51], focusing on the removal both of fluoride ions and As(V). In addition, a magnesium-activated carbon composite (Mg–AC) was tested for the efficient adsorption of Zn(II) and Cd(II) ions [52]. Moreover, activated carbon modified with MgSiO₃ (magnesium silicate) was applied to remove Pb(II) [53]. In recent studies [54,55], the presence of magnesium has shown a significant effect on arsenic removal. Mg²⁺ ions exhibit a corresponding affinity with As that enhances the adsorption effect of the modified activated carbon. In conclusion, the combination of such additives, i.e., La, Mg, and Si, for the alteration of activated carbon derived from low-cost raw materials, with the aim of increasing its surface area, its selectivity to specific pollutants and its effectiveness, has not been used in the recent literature.

Therefore, a hybrid material already synthesized in our previous research [43] and applied with great success in the removal of Cr(VI) from water, combining the benefits of Mg, Si, La and AC (hereafter Mg-Si-La@AC), is examined in this study regarding its potential effectiveness in removing As(III). FTIR and SEM techniques were applied to study both the structure and morphology of Mg-Si-La@AC. Moreover, the effects of numerous parameters (pH, As(III) concentration, dosage of adsorbent and contact time) were studied. Isotherm, kinetic, thermodynamic and regeneration studies were performed to describe and evaluate the adsorption that occurred.

2. Materials and Methods

2.1. Materials

For 100 mg of As(III)/L solution, an appropriate amount of sodium metarsenite (AsNaO₂) (Merck) (0.1733 g) was dissolved in 1 L of deionized water and kept in a cool place for further use. For the modification of activated carbon, lanthanum chloride heptahydrate

98% (LaCl₃) (Merck), MgO (PMS2 pure magnesia) and silicon dioxide (SiO₂) (Merck) were used. The pH was adjusted accordingly by utilizing a HCl solution of 37% (Panreac) or NaOH pellets ACS ≥ 97.0%, (Sigma-Aldrich, St. Louis, MO, USA) (0.01–0.1 M).

Synthesis of Hybrid Mg-Si-La@AC

The Mg-Si-La@AC was synthesized via the modification of activated carbon produced by coconut shells, with magnesium, silicate and lanthanum. The detailed procedure is given in previous studies published by our group [43,44]. In brief, 5 g of AC that was previously activated by 2 M KOH at 25° C for 24 h was added to three beakers of 25 mL of distilled water, each containing 1.8 g of LaCl₃, 0.8 g of MgO or 0.6 g of SiO₂, respectively, and mixed for 1 h at 25° C and sonicated for 2 h. After filtering and rinsing with distilled water, the samples produced (i.e., La@AC, Mg@AC and Si@AC, respectively) were dried overnight at 333 K. In order to produce the composite Mg-Si-La@AC, the calcination of the servings of the above samples took place at 773 K for 5 h. Finally, all samples were kept at room temperature until use.

2.2. Adsorption Experiments

To carry out the experiments, 10 mL of a constant concentration of arsenic solution was added to 15 mL falcon tubes, followed by the addition of a fixed amount of adsorbent under constant temperature. A Trayster overhead shaker and Loopster rotator were used to stir the suspension at 80 rpm. The experimental parameters considered were the solution pH, which was 4.0–9.0, the initial As(III) concentration, which was 25–500 µg/L, the adsorbent's dose, which varied from 0.5 to 3.0 g/L, and the contact time, which ranged from 10 min up to 360 min for kinetics and up to 24 h when aiming to reach equilibrium. The above-mentioned parameters were measured in the filtrate obtained after filtering the collected samples through a 0.45 µm nylon filter. The following Equation (1) was used to calculate the percentage removal (% R) of As(III):

$$R(\%) = \left(\frac{C_0 - C_f}{C_0} \right) \times 100\% \quad (1)$$

where C_0 is the initial and C_f is the final (residual) As(III) concentration (µg/L).

Moreover, Equation (2) was used for the determination of the adsorbent's adsorption capacity (Q_e) (µg/g):

$$Q_e = \frac{(C_0 - C_e) \times V}{m} \quad (2)$$

where C_e = As(III) concentration (µg/L) at equilibrium, V = volume of solution (L), and m = mass (g) of the adsorbent.

2.2.1. Adsorption Isotherms

For the adsorption isotherms, the results were fitted to the Langmuir and Freundlich isothermal models, which are the commonly used and easiest to apply models.

The Langmuir model is expressed as Equation (3) [56] and determines the relationship between the concentration of the adsorbate in the solid phase (Q_e) and the uptake to the equilibrium liquid concentration:

$$Q_e = \frac{Q_m K_L C_e}{1 + K_L C_e} \quad (3)$$

where Q_m is the maximum adsorption capacity (µg/L), and K_L is the energy of the As(III) (L/µg) adsorption.

Furthermore, according to the Langmuir theory, the adsorption capacity of the adsorbent is partial (Q_m), with the adsorbate forming a monolayer on the surface of the adsorbent; hence, the interface between the adsorbed molecules is almost non-existent [51].

On the other hand, the Freundlich model [57] describes the relationship between the equilibrium As(III) concentrations ($\mu\text{g/L}$) and the uptake capacities Q_e ($\mu\text{g/g}$) of the adsorbent; it is stated as Equation (4):

$$Q_e = K_F C_e^{1/n} \quad (4)$$

where K_F ($(\mu\text{g/g})(\text{L}/\mu\text{g})^{1/n}$) is a constant related to the adsorption capacity and $1/n$ is a constant related to the intensity of the adsorption or surface heterogeneity:

- $1/n = 0$ means heterogeneity;
- $1/n < 1$ means a normality; and
- $1/n > 1$ designates a cooperativeness.

2.2.2. Kinetics

Two kinetic models were examined to fit the kinetics of As(III) adsorption; PFO (pseudo-first-order) and PSO (pseudo-second-order) models. These models are the most widely used models in adsorption experiments. Then, the calculated kinetic parameters of adsorption were analyzed in order to evaluate the adsorption rate, as well as to identify the possible reaction mechanism. The PFO model used is expressed as Equation (5):

$$Q_t = Q_e \left(1 - e^{-k_1 t}\right) \quad (5)$$

where Q_e = amount of As(III) adsorbed at equilibrium ($\mu\text{g/g}$), Q_t = amount of As(III) adsorbed at time t ($\mu\text{g/g}$), k_1 = rate constant of the PFO model ($1/\text{min}$), and t = time (min).

The PSO model used for the data analysis is expressed as Equation (6):

$$Q_t = \frac{k_2 Q_e^2 t}{1 + k_2 Q_e t} \quad (6)$$

where Q_e = amount of As(III) adsorbed at equilibrium ($\mu\text{g/g}$), Q_t = amount of As(III) adsorbed at time t ($\mu\text{g/g}$), k_2 = rate constant of the PSO ($\text{g}/(\mu\text{g min})$), and t = time (min).

2.3. Arsenic Determination

After adsorption, water samples were collected from the supernatant of each falcon tube, filtered through a $0.45 \mu\text{m}$ nylon membrane filter, and saved for immediate determination. The initial and residual arsenic concentrations were then determined using an atomic absorption spectrometer (Varian Zeeman AA240Z with GTA 120; Hansen Way Palo Alto, CA, USA) coupled with a graphite furnace (graphite furnace-AAS). The detection limit of the AAS was $1 \mu\text{g/L}$. The values obtained were converted to residual concentrations by corresponding the absorbance to the standard curve of As. To confirm the results and the accuracy of the procedure, the experiments were initially performed in triplicate and each sample obtained was measured three times. Data were expressed as mean trace element values \pm standard deviation.

2.4. Thermodynamics

The thermodynamic parameters, such as the change in Gibbs free energy (ΔG^0 , kJ/mol), enthalpy (ΔH^0 , kJ/mol) and entropy (ΔS^0 , $\text{kJ/mol}\cdot\text{K}$), were calculated in order to estimate the adsorption process and determine the possible spontaneous nature. Consequently, for this reason, several indicative temperatures (298, 308, 318, and 338 K) were tested and the following equations were used to calculate the thermodynamic parameters [58]:

$$K_c = \frac{C_s}{C_e} \quad (7)$$

$$\Delta G^0 = -RT \ln(K_c) \quad (8)$$

$$\Delta G^0 = \Delta H^0 - T\Delta S^0 \quad (9)$$

$$\ln(K_c) = \left(-\frac{\Delta H^0}{R} \right) + \frac{\Delta S^0}{R} \quad (10)$$

ΔG^0 was given from Equation (8), and for the calculation of the ΔH^0 and ΔS^0 values, the plot of $\ln(K_c)$ versus $1/T$ (Equation (10)) was applied. The relative slope and intercept resulted in the values.

2.5. Characterization Techniques

To study the surface of the adsorbent, the most common techniques were applied. Therefore, SEM (Scanning Electron Microscopy) (Jeol JSM-6390 LV, Musashino, Akishima, Tokyo 196-8558, Japan, scanning electron microscope), equipped with an EDS (energy-dispersive X-ray) system, was used for surface element analysis; thus, a focused electron beam was used to scan the surface. The results obtained from our electron microscope are given in the form of images of morphological content in relation to the surface and phase distribution, as well as the characteristic X-ray spectra or visualization of the distribution of various data on the surface of the sample. In addition, FT-IR (Fourier-Transform Infrared Spectroscopy) (Perkin Elmer, New York, NY, USA) and BET (Brunauer, Emmett and Teller) analysis software (Quantachrome NovaWin; Data Acquisition and Reduction) for NOVA instruments 1994-2012, Quantachrome instruments version 11-02, using computer-controlled nitrogen gas adsorption analyzer, were used to determine the specific surface area, including the pore size distribution. BET theory has the effect of determining the molecules, calculated through experimental experience, that are needed to form a single layer, excluding the fact that it is impossible to create one.

3. Results and Discussion

3.1. Characterization of Mg-Si-La@AC

The nitrogen adsorption and desorption isotherms for Mg-Si-La@AC versus the relative pressure (P/P_0) are shown in Figure 1. As depicted, Mg-Si-La@AC shows a Type IV model of isotherm with hysteresis loops [59], according to the IUPAC (International Union of Pure and Applied Chemistry), ascertaining their mesoporous structure. The BET-specific surface area values, median BJH (Barrett–Joyner–Halenda) pore size and pore volume of Mg-Si-La@AC are given in Table 1.

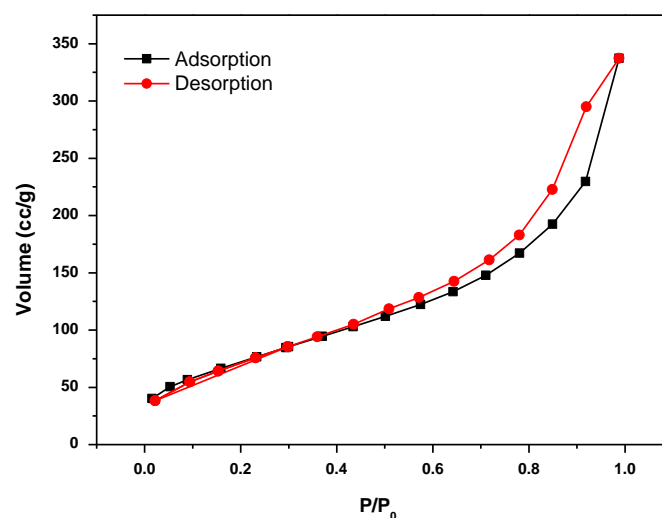
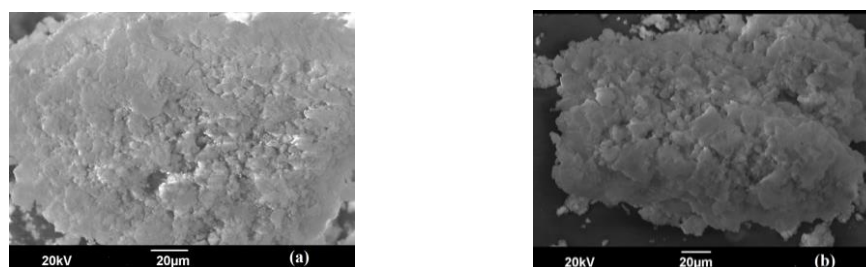


Figure 1. N₂ adsorption/desorption isotherms of Mg-Si-La@AC adsorbent against relative pressure (P/P_0) from 0 to 1.

Table 1. Physical properties of Mg-Si-La@AC.

Parameters	Mg-Si-La@AC
BET Surface area, S_{BET} (m^2/g)	271.46
Micropore volume, V_{micro} (cm^3/g)	0.006
Total pore volume, V_T (cm^3/g)	0.521

According to the determinations, the BET surface area of Mg-Si-La@AC was calculated to be $271.46 m^2/g$, the respective total pore volume was $0.006 cm^3/g$, and the micropore volume was measured as $0.521 cm^3/g$, which show that Mg-Si-La@AC is practically efficient for adsorption, providing a high surface area. The morphology and structure of the modified activated carbon were observed using SEM images. As shown in Figure 2a, Mg-Si-La@AC shows a porous structure with cavities, possibly due to the carbonization stage that takes place during synthesis. Nasri et al. have also observed more developed carbon pore structures, which were synthesized from coconut shell using two-step CO_2 activation [60]. In Figure 2b, it is shown that these pores are filled with As after the adsorption experiments.

**Figure 2.** SEM image of Mg-Si-La@AC (a) pre and (b) post arsenic adsorption.

In addition, an EDS analysis of Mg-Si-La@AC pre and post As(III) adsorption was conducted, as shown in Figure 3 and Table 2. According to the results, Mg, Si and La were detected on the activated carbon surface, confirming its amendment. After the adsorption of As(III), a higher percentage of oxygen content and the appearance of As were observed, which is probably due to the addition of sodium metarsenite ($AsNaO_2$) and its binding. Additionally, a decrease in the Mg, Si and La content was detected, which probably contributed to the removal of As.

Table 2. SEM/EDS analysis of Mg-Si-La@AC pre and post As(III) adsorption.

Element	Mg-Si-La@AC	Mg-Si-La@AC_As
	Content% (<i>w/w</i>)	
La	3.59	2.46
Mg	6.07	4.79
C	12.64	9.04
Si	8.26	7.56
P	0.79	1.04
O	68.65	74.14
As	0	0.96

The FTIR spectra of Mg-Si-La@AC pre and post As(III) adsorption are shown in Figure 4. As can be seen, the spectra are similar, with a slight change in the intensity and formation of characteristic new bands or the disappearance of others. Specifically, the first broad and stretched peak was obtained at 3395 and $3385 cm^{-1}$ for the spectra of Mg-Si-La@AC pre and post As(III) adsorption, respectively, and corresponds to the characteristic symmetric and asymmetric stretching vibration of the O–H hydroxyl group, which ranges from $3200–3600 cm^{-1}$ [61]. Furthermore, the peaks at $2217–1936/2224–1945 cm^{-1}$

and $1508\text{--}1415/1501\text{--}1425\text{ cm}^{-1}$ were related to C–H, --C=C-- (carbonyl) and C–C aromatic stretching, corresponding to the IR pre and post adsorption [61]. The ranging from $600\text{--}740\text{ cm}^{-1}$ corresponds to MgO stretching vibrations [43], La_2O_3 [61] and to the bending of the O–Si–O [20], confirming the modification of AC with Mg, Si and La. Observing the post-adsorption spectra, there is a new absorption peak that appears at 863 cm^{-1} and can be attributed, according to the literature, to the As–O–La bond [61,62]. In addition, a more intense peak at 738.5 cm^{-1} , post adsorption, corresponds to As–O–Mg vibrations [63]. This proves that As(III) is adsorbed on the Mg–Si–La@AC surface and, indeed, that La and Mg contribute to the binding of arsenic, as was hypothesized earlier in the elemental analysis (Table 2).

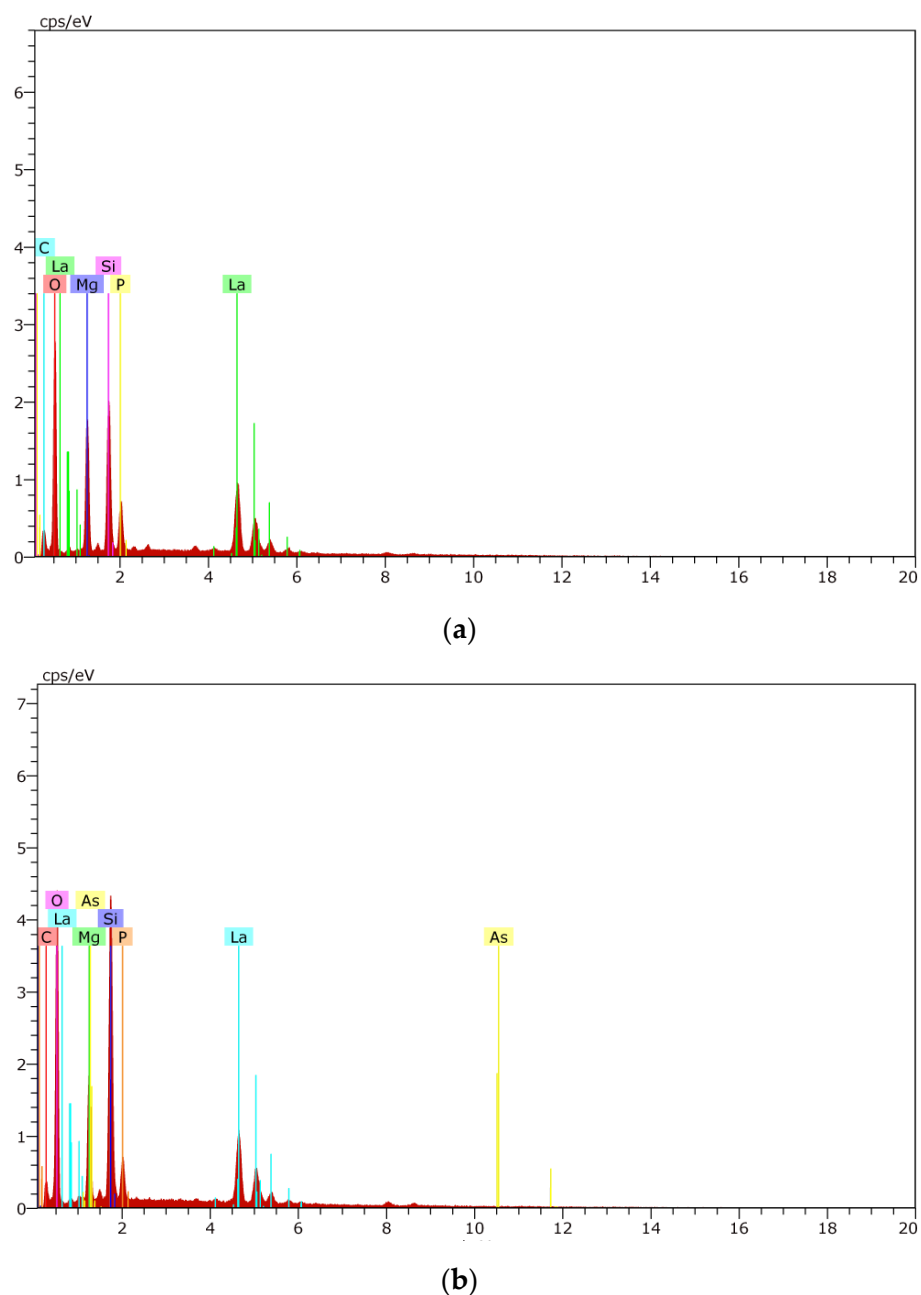


Figure 3. Elemental spectra (a) pre and (b) post arsenic adsorption on Mg–Si–La@AC, detected using SEM/EDS analysis.

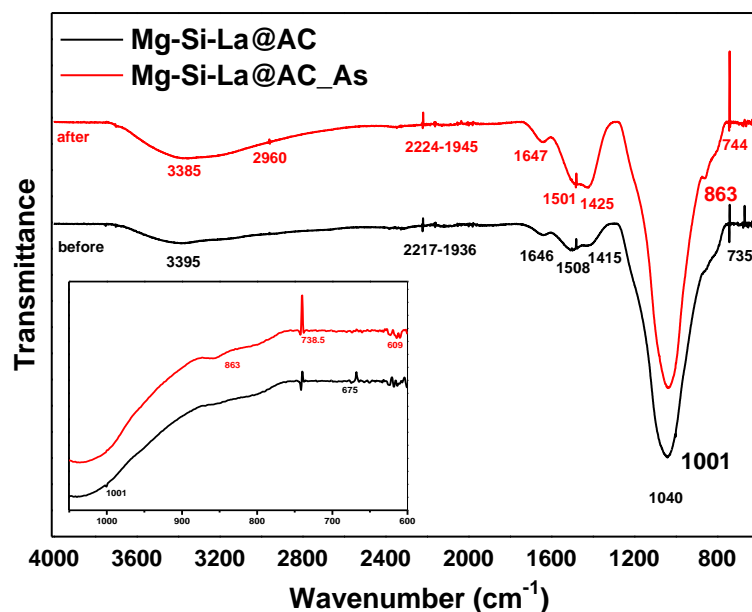


Figure 4. FTIR spectra pre and post arsenic adsorption on Mg-Si-La@AC.

3.2. Batch Adsorption Experiments

Effect of Modification of Activated Carbon

As shown in Figure 5, as the modification of the activated carbon increases, so does its effectiveness in the adsorption of As(III). For instance, when activated carbon is modified with silicon (Si@AC) or lanthanum (La@AC), no significant improvement is observed; however, when modified with magnesium, the performance of this combined material (Mg-Si-La@AC) increases. What follows is that the presence of magnesium contributes significantly to the removal of As(III). This is confirmed both by the elemental analysis presented in Table 2, where the Mg content decreases after As(III) adsorption, and by the appearance of the peak in the FTIR corresponding to the As–O–Mg vibrations (Figure 4). In recent studies [54,55], the presence of magnesium has been shown to have a significant effect on arsenic removal. The Mg^{2+} ions contained in MgO, as demonstrated via EDS analysis and FTIR, are successfully deposited on the surface of the activated carbon and thus exhibit a corresponding affinity with As that enhances the adsorption effect of the modified activated carbon. To conclude, the Mg-Si-La@AC adsorbent is found to be optimal for further study.

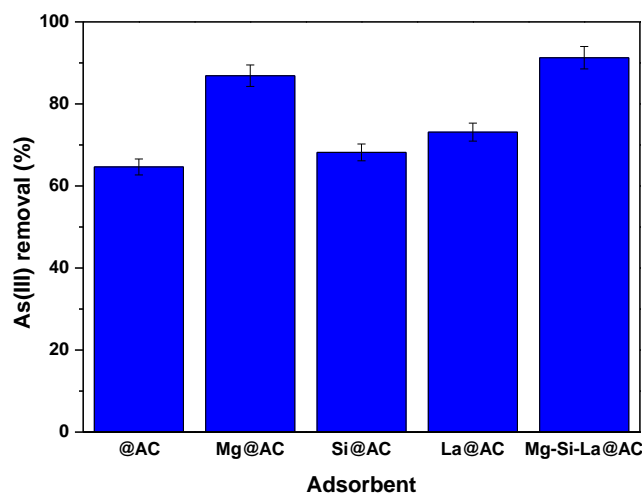


Figure 5. Effect of modification of activated carbon on the removal of As(III). C_0 100 $\mu\text{g/L}$, dose 1.5 g/L, pH 7.0, 24 h.

3.3. Effect of Dosage and Initial Solution pH

The potential of Mg-Si-La@AC to be applied in As(III) removal was evaluated by examining the effect of the adsorbent dosage and initial pH. The pH values tested were in the range of 4.0–9.0. These values were chosen for two reasons. Firstly, the pH of groundwater typically ranges between 6.0–8.5 [15]; secondly, according to the literature [64], As(III) is better removed at pH values of 4.0–6.0, while As(V) is better removed at pH values of 4.0–8.0. As depicted in Figure 6, by increasing the adsorbent's dosage, the removal rate of As(III) is also increased, from 49% (by 0.5 g/L) to 93% (by 1.5 g/L) at pH 7.0 (Figure 6a). Therefore, pH 7.0 was found to be optimal, as for a dose of 1.5 g/L, the residual As(III) concentration (8.82 $\mu\text{g/L}$) remains below the legislation limit of 10 $\mu\text{g/L}$ (Figure 6b). pH 7.0 was also found to be the most efficient for As(III) removal according to the literature [38,63,65]. Moreover, the pH_{pzc} (point of zero charge) of Mg-Si-La@AC was previously measured [44] using the pH drift method and measured as 7.72. pH_{pzc} is the critical point at which the surface charge of the adsorbent changes from positive to negative, affecting the adsorbent–adsorbed substance interface. Therefore, at $\text{pH} < \text{pH}_{\text{pzc}}$ (i.e., $7 < 7.72$), the surface of Mg-Si-La@AC is positively charged, giving it the ability to attract arsenic anions via electrostatic interaction. Furthermore, at pH 7.0, As(III), with a $\text{pK}_{\text{a}1}$ of 9.22, exists mainly as non-ionic H_3AsO_3 [66]; therefore, at this pH, As(III) adsorption is less sensitive to pH [67] and the adsorption of non-ionized As(III) occurs only through a ligand exchange reaction [68].

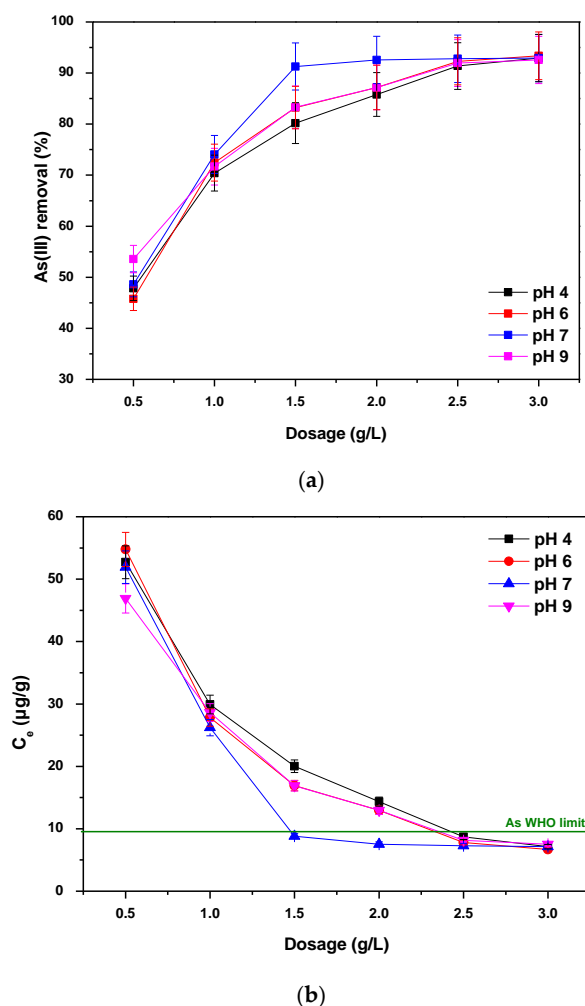


Figure 6. Effect of Mg-Si-La@AC dosage and solution pH, in terms of (a) removal % and (b) C_e ($\mu\text{g/L}$); C_0 100 $\mu\text{g/L}$, $T = 298$ K, 24 h.

3.4. Adsorption Isotherms

Langmuir and Freundlich isotherm models were used in this study to evaluate the adsorption equilibrium data of As(III) on Mg-Si-La@AC at the optimal conditions obtained from the above experiments. These are the most commonly applied models described by two parameters. As presented in Figure 7, the Langmuir isotherm model was found to better fit the adsorption ($R^2 = 0.98$) and a calculated adsorption capacity (Q_m) of 322 $\mu\text{g/g}$. On the contrary, the results did not fit well to the Freundlich model (as $R^2 = 0.88$). Hence, it could be assumed that the monolayer adsorption of As(III) took place on the homogeneous surface of the Mg-Si-La@AC adsorbent (according to the Langmuir model), with the adsorption occurring at a fixed number of sites without lateral interaction between the adsorbent and adsorbate molecule, with the energy of adsorption remaining constant [69]. The comparative fitting parameters (calculated from Equations (3) and (4)) are tabulated in Table 3.

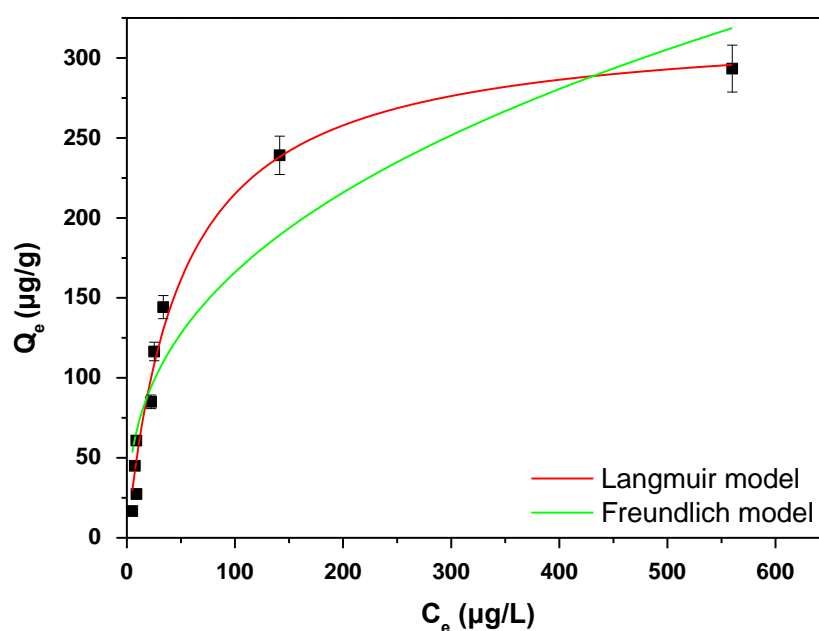


Figure 7. Langmuir and Freundlich isotherm models; dose 1.5 g/L Mg-Si-La@AC (1.5 g/L), pH 7.0, $T = 298\text{ K}$, 24 h.

Table 3. Constants of Langmuir and Freundlich isotherm models for the adsorption of As(III) onto Mg-Si-La@AC (1.5 g/L), pH 7.0, $T = 298\text{ K}$, 24 h.

Langmuir Isotherm Model		
Q_m ($\mu\text{g/g}$)	K_L ($\text{L}/\mu\text{g}$)	R^2
322	0.020	0.9898
Freundlich isotherm model		
$1/n$	K_F ($\mu\text{g/g})(\text{L}/\mu\text{g})^{1/n}$	R^2
0.3785	29.04	0.8780

3.5. Effect of Contact Time–Kinetic Models

Figure 8 presents the effect of the contact time varying from 5 to 1440 (24 h). According to the results, to increase the removal rate of As(III) and the relative cost-effectiveness of adsorption, 4 h was considered to be the optimal contact time for the experiments. In addition, adsorption kinetics was used to appreciate the adsorption rate and the possible mechanism controlling the whole process. To interpret the adsorption kinetics of As(III) on AC-Si-Mg-La, the PFO and the PSO kinetics models were applied to evaluate the

experimental data (Figure 9). From the results presented in Table 4 it appears that the procedure best followed the PSO model, as the correlation coefficient for the PSO model was calculated as $R^2 = 0.93$ and the relative one for the PFO model was only 0.80. The PSO model was used to define the kinetics of slow adsorption, predicting the long-term adsorption equilibrium. The PSO kinetic model was also found to be the most applicable in recent studies for arsenic removal [14,70].

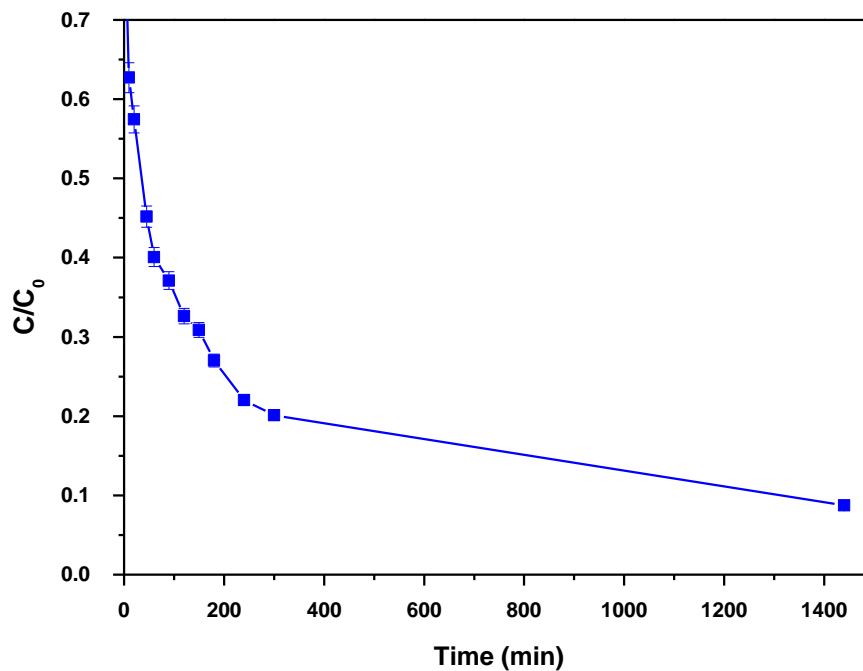


Figure 8. Effect of time on As(III) adsorption onto Mg-Si-La@AC (1.5 g/L), pH 7.0, $T = 298$ K.

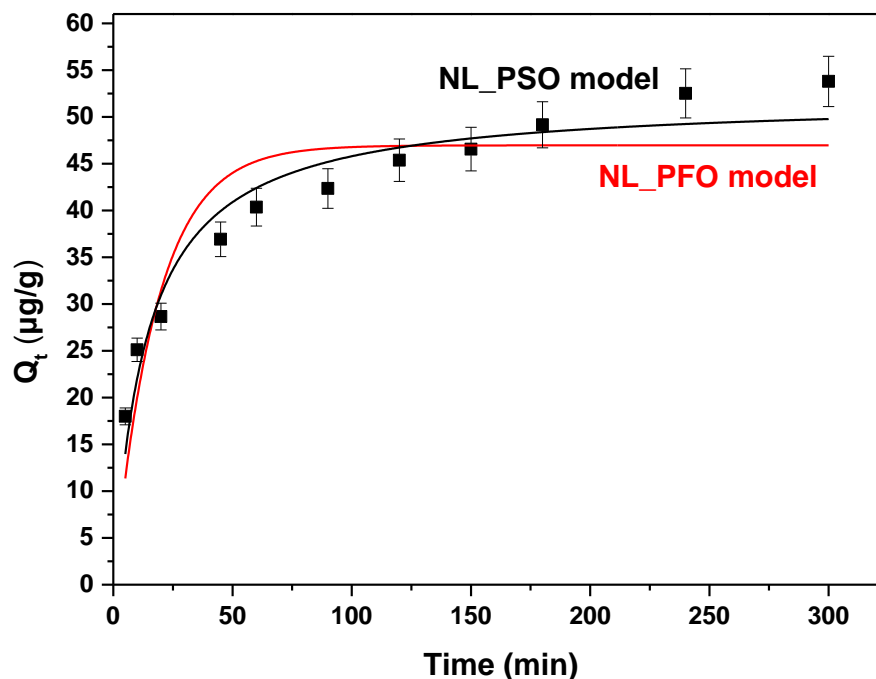


Figure 9. Non-linear kinetic models PFO and PSO for the adsorption of As(III) onto Mg-Si-La@AC (1.5 g/L), pH 7.0, $T = 298$ K.

Table 4. PFO and PSO kinetic parameters model for the adsorption of As(III) onto Mg-Si-La@AC (1.5 g/L), pH 7.0, $T = 298$ K.

Pseudo-First-Order Kinetic Model (PFO)			
$Q_{e\text{-exp}}$ ($\mu\text{g/g}$)	K_1 (L/ $\mu\text{g}\cdot\text{min}$)	$Q_{e\text{-cal}}$ ($\mu\text{g/g}$)	R^2
61.47	0.0554	46.96	0.8008
Pseudo-second order kinetic model (PSO)			
$Q_{e\text{-exp}}$ ($\mu\text{g/g}$)	K_2 (L/ $\mu\text{g}\cdot\text{min}$)	$Q_{e\text{-cal}}$ ($\mu\text{g/g}$)	R^2
61.47	0.0014	52.04	0.9318

3.6. Thermodynamics

Temperature is a variable that affects the adsorption process, and its effect on the adsorption of As(III) was observed at different temperatures, such as 298, 308, 318 and 338 K. For the determination of the thermodynamic parameters, the Equations (7–10) were used and the results are presented in Table 5. The values of ΔH^0 and ΔS^0 were obtained by analyzing the plot of $\ln(K_c)$ versus $1/T$ [71], providing a R^2 value of 0.9684. The values of ΔG^0 were calculated to be negative, indicating that the process is spontaneous. The ΔH^0 value for As(III) removal was determined to be 55.114 kJ/mol, demonstrating the endothermic nature of the adsorption process. Moreover, the positive ΔS^0 (0.1916 kJ/mol·K) was due to the increased randomness of adsorbed substances at the interface of the solid and the solute during the adsorption [72].

Table 5. Thermodynamic parameters for the adsorption of As(III) onto Mg-Si-La@AC; C_0 100 $\mu\text{g/L}$, dose 1.5 g/L, pH 7.0, 3 h.

T (K)	ΔG^0 (kJ/mol)	ΔH^0 (kJ/mol)	ΔS^0 (kJ/mol·K)	R^2
298	−1.969			
308	−3.884	55.114	0.1916	0.9684
318	−5.800			
338	−9.631			

3.7. Regeneration Study

Another important factor in the study of adsorption is the reusability of the adsorbents; thus, recycling studies were carried using similar experimental conditions, which were applied in each cycle (i.e., initial As(III) concentration of 100 $\mu\text{g/L}$, dose of 1.5 g/L, pH 7.0), using 0.01 M of NaOH. As shown in Figure 10, only a 20% reduction in the adsorption capacity after four regeneration cycles of the process was observed (from 92.8% at the first cycle to 70.6% at the fourth). Therefore, this study showed that the Mg-Si-La@AC adsorbent could be reused for four cycles, with the efficacious regenerate providing an approximately 93% removal of As(III) after the first cycle and approximately 71% removal after the fourth cycle.

3.8. Comparison with Literature

Table 6 provides a comparison between Mg-Si-La@AC and other modified activated carbons found in the literature for removing As(III). A neutral pH (7.0) was found to be optimal in most of the cases analyzed here. The initial As concentration used in most experiments (i.e., 10 mg/L) and the relative dosages of adsorbents (even 50 g/L) were generally much higher than those used in the present study. Regeneration studies showed that the adsorbents could be regenerated and reused up to 4–5 cycles. Finally, the removal rate of As(III) (93%) using Mg-Si-La@AC was high compared to the corresponding literature.

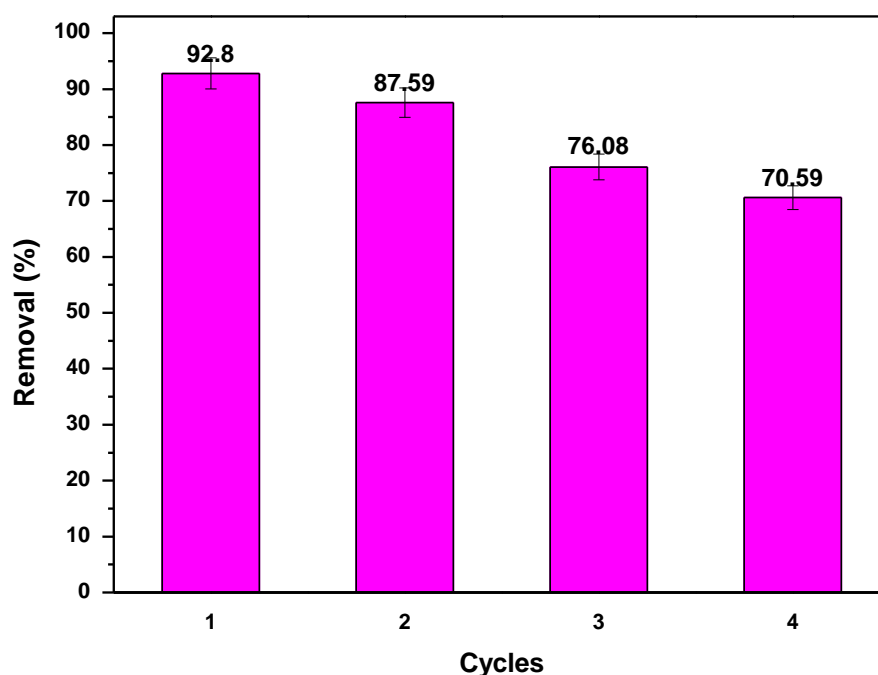


Figure 10. Regeneration study of four adsorption-desorption cycles.

Table 6. Comparison of the adsorption effect of arsenic with other modified activated carbons found in the literature.

Adsorbent	[As] ₀ (mg/L)	Dosage (g/L)	pH _{init}	Adsorption Capacity (mg/g)	Removal %	Cycles	Ref.
Fe-Zr@AC ¹	1.0	3.0	7.0	1.206	86	5	[73]
AC-Tamarix ²	10.0	3.0	7.0	37.313	96	-	[74]
MgO/AC/Fe ₃ O ₄ ³	6.0	0.13	7.0	1.166	97	5	[75]
AGSC ⁴	0.4	5.0	6.0	0.192	93	5	[76]
ACF ⁵	2.0	0.5	6.0	8.651	74	-	[77]
ZrO ₂ /AC ⁶	10.0	50.0	5.0	64.0	90	4	[78]
Mg-Si-La@AC ⁷	0.1	1.5	7.0	0.322	93	4	this study

¹ Iron-zirconium-modified activated carbon; ² Activated carbon adsorbent prepared from Tamarix tree leaves; ³ Fe₃O₄/MgO/Activated carbon composite; ⁴ Nanoporous activated garlic stem carbon; ⁵ Fe- and HNO₃-modified activated carbon fiber; ⁶ Zirconia-modified activated carbon; ⁷ Magnesium/Silica/Lanthanum@Activated Carbon.

4. Conclusions

The objective of this study was to observe the application of Magnesium/Silica/Lanthanum@Activated Carbon (Mg-Si-La@AC) for the first time in the removal of As(III) from water. BET, FTIR and SEM techniques were used for the characterization of the material. Therefore, the BET surface area, total pore volume, and micropore volume of Mg-Si-La@AC were measured to be 271.46 m²/g, 0.006 cm³/g and 0.52 cm³/g, respectively. According to the results, Mg, Si and La were detected on the activated carbon surface, confirming its amendment. Observing the post-adsorption FTIR spectra, new absorption peaks appeared at 863 cm⁻¹ and 738.5 cm⁻¹, and could be attributed to As-O-La and As-O-Mg bonds, indicating that As(III) is adsorbed on the Mg-Si-La@AC surface.

Furthermore, several parameters were examined to evaluate the process. Hence, an optimal dose of 1.5 g/L and pH 7 were selected, resulting in a residual As concentration < 10 µg/L. In addition, 4 h was selected as the optimal time for the experiments and the procedure best followed the PSO kinetic model. The maximum adsorption capacity was determined to be 322 µg/g at pH 7, according to the Langmuir isotherm model. Moreover, thermodynamics

studies showed that, by increasing the temperature from 25 to 65 °C, the removal capacity was increased by 80%. Finally, regeneration studies showed that the Mg-Si-La@AC adsorbent could be reused for four cycles with only a 20% decrease in the adsorption capacity.

Author Contributions: Conceptualization, A.K.T. and G.Z.K.; methodology, A.K.T. and G.Z.K.; validation, G.Z.K.; formal analysis, A.K.T. and G.Z.K.; investigation, A.K.T. and G.Z.K.; resources, A.K.T. and G.Z.K.; data curation, A.K.T.; writing—original draft preparation, A.K.T.; writing—review and editing, A.K.T. and G.Z.K.; visualization, A.K.T. and G.Z.K.; supervision, A.K.T. and G.Z.K. All authors have read and agreed to the published version of the manuscript.

Funding: This research received no external funding.

Institutional Review Board Statement: Not applicable.

Informed Consent Statement: Not applicable.

Data Availability Statement: All data analyzed during this study are included in this published article.

Acknowledgments: We acknowledge support of this work by the project “Advanced Nanostructured Materials for Sustainable Growth: Green Energy Production/Storage, Energy Saving and Environmental Remediation” (TAEDR-0535821) which is implemented under the action “Flagship actions in interdisciplinary scientific fields with a special focus on the productive fabric” (ID 16618), Greece 2.0—National Recovery and Resilience Fund and funded by European Union NextGenerationEU. The authors, also thank Olina Makrogianni for taking some characterization measurements.

Conflicts of Interest: The authors declare no conflict of interest.

References

1. Li, P.; Karunanidhi, D.; Subramani, T.; Srinivasamoorthy, K. Sources and Consequences of Groundwater Contamination. *Arch. Environ. Contam. Toxicol.* **2021**, *80*, 1–10. [[CrossRef](#)]
2. Bundschuh, J.; Armienta, M.A.; Morales-Simfors, N.; Alam, M.A.; López, D.L.; Delgado Quezada, V.; Dietrich, S.; Schneider, J.; Tapia, J.; Sracek, O.; et al. Arsenic in Latin America: New Findings on Source, Mobilization and Mobility in Human Environments in 20 Countries Based on Decadal Research 2010–2020. *Crit. Rev. Environ. Sci. Technol.* **2020**, *51*, 1727–1865. [[CrossRef](#)]
3. Rahaman, M.S.; Mise, N.; Ichihara, S. Arsenic Contamination in Food Chain in Bangladesh: A Review on Health Hazards, Socioeconomic Impacts and Implications. *Hyg. Environ. Health Adv.* **2022**, *2*, 100004. [[CrossRef](#)]
4. McKay, G.; Otterburn, M.S.; Sweeney, A.G. The Removal of Colour from Effluent Using Various Adsorbents: Some Preliminary Economic Considerations. *J. Soc. Dye. Colour.* **1978**, *94*, 357–360. [[CrossRef](#)]
5. Shaji, E.; Santosh, M.; Sarath, K.V.; Prakash, P.; Deepchand, V.; Divya, B.V. Arsenic Contamination of Groundwater: A Global Synopsis with Focus on the Indian Peninsula. *Geosci. Front.* **2021**, *12*, 101079. [[CrossRef](#)]
6. Ur Rehman, H.; Ahmed, S.; Ur Rahman, M.; Mehmood, M.S. Arsenic Contamination, Induced Symptoms, and Health Risk Assessment in Groundwater of Lahore, Pakistan. *Environ. Sci. Pollut. Res.* **2022**, *29*, 49796–49807. [[CrossRef](#)]
7. Subhani, M.; Mustafa, I.; Alamdar, A.; Katsoyiannis, I.A.; Ali, N.; Huang, Q.; Peng, S.; Shen, H.; Eqani, S.A.M.A.S. Arsenic Levels from Different Land-Use Settings in Pakistan: Bio-Accumulation and Estimation of Potential Human Health Risk via Dust Exposure. *Ecotoxicol. Environ. Saf.* **2015**, *115*, 187–194. [[CrossRef](#)] [[PubMed](#)]
8. Pezeshki, H.; Hashemi, M.; Rajabi, S. Removal of Arsenic as a Potentially Toxic Element from Drinking Water by Filtration: A Mini Review of Nanofiltration and Reverse Osmosis Techniques. *Heliyon* **2023**, *9*, e14246. [[CrossRef](#)]
9. Mazumder, D.N.G. Health Effects of Chronic Arsenic Toxicity. In *Handbook of Arsenic Toxicology*; Elsevier: Amsterdam, The Netherlands, 2023; pp. 151–192. [[CrossRef](#)]
10. Fatoki, J.O.; Badmus, J.A. Arsenic as an Environmental and Human Health Antagonist: A Review of Its Toxicity and Disease Initiation. *J. Hazard. Mater. Adv.* **2022**, *5*, 100052. [[CrossRef](#)]
11. Genchi, G.; Lauria, G.; Catalano, A.; Carocci, A.; Sinicropi, M.S. Arsenic: A Review on a Great Health Issue Worldwide. *Appl. Sci.* **2022**, *12*, 6184. [[CrossRef](#)]
12. World Health Organization European Standards for Drinking-Water. *Am. J. Med. Sci.* **1970**, *242*, 56.
13. Jadhav, S.V.; Bringas, E.; Yadav, G.D.; Rathod, V.K.; Ortiz, I.; Marathe, K.V. Arsenic and Fluoride Contaminated Groundwaters: A Review of Current Technologies for Contaminants Removal. *J. Environ. Manag.* **2015**, *162*, 306–325. [[CrossRef](#)]
14. Katsoyiannis, I.A.; Tzollas, N.M.; Tolkou, A.K.; Mitrakas, M.; Ernst, M.; Zouboulis, A.I. Use of Novel Composite Coagulants for Arsenic Removal from Waters—Experimental Insight for the Application of Polyferric Sulfate (PFS). *Sustainability* **2017**, *9*, 590. [[CrossRef](#)]
15. Meez, E.; Tolkou, A.K.; Giannakoudakis, D.A.; Katsoyiannis, I.A.; Kyzas, G.Z. Activated Carbons for Arsenic Removal from Natural Waters and Wastewaters: A Review. *Water* **2021**, *13*, 2982. [[CrossRef](#)]

16. Cañas Kurz, E.E.; Hellriegel, U.; Figoli, A.; Gabriele, B.; Bundschuh, J.; Hoinkis, J. Small-Scale Membrane-Based Arsenic Removal for Decentralized Applications—Developing a Conceptual Approach for Future Utilization. *Water Res.* **2021**, *196*, 116978. [[CrossRef](#)]
17. Worou, C.N.; Chen, Z.L.; Bacharou, T. Arsenic Removal from Water by Nanofiltration Membrane: Potentials and Limitations. *Water Pract. Technol.* **2021**, *16*, 291–319. [[CrossRef](#)]
18. Nur, T.; Loganathan, P.; Ahmed, M.B.; Johir, M.A.H.; Nguyen, T.V.; Vigneswaran, S. Removing Arsenic from Water by Coprecipitation with Iron: Effect of Arsenic and Iron Concentrations and Adsorbent Incorporation. *Chemosphere* **2019**, *226*, 431–438. [[CrossRef](#)] [[PubMed](#)]
19. Zama, E.F.; Li, G.; Tang, Y.T.; Reid, B.J.; Ngwabie, N.M.; Sun, G.X. The Removal of Arsenic from Solution through Biochar-Enhanced Precipitation of Calcium-Arsenic Derivatives. *Environ. Pollut.* **2022**, *292*, 118241. [[CrossRef](#)]
20. Dudek, S.; Kołodyńska, D. Arsenate Removal on the Iron Oxide Ion Exchanger Modified with Neodymium(III) Ions. *J. Environ. Manag.* **2022**, *307*, 114551. [[CrossRef](#)]
21. Saleh, T.A.; Mustaqeem, M.; Khaled, M. Water Treatment Technologies in Removing Heavy Metal Ions from Wastewater: A Review. *Environ. Nanotechnol. Monit. Manag.* **2022**, *17*, 100617. [[CrossRef](#)]
22. Shankar, S.; Shankar, U. Shikha Arsenic Contamination of Groundwater: A Review of Sources, Prevalence, Health Risks, and Strategies for Mitigation. *Sci. World J.* **2014**, *2014*, 304524. [[CrossRef](#)] [[PubMed](#)]
23. Pang, X.; Sellaoui, L.; Franco, D.; Dotto, G.L.; Georgin, J.; Bajahzar, A.; Belmabrouk, H.; Ben Lamine, A.; Bonilla-Petriciolet, A.; Li, Z. Adsorption of Crystal Violet on Biomasses from Pecan Nutshell, Para Chestnut Husk, Araucaria Bark and Palm Cactus: Experimental Study and Theoretical Modeling via Monolayer and Double Layer Statistical Physics Models. *Chem. Eng. J.* **2019**, *378*, 122101. [[CrossRef](#)]
24. Wang, X.; Xu, Q.; Zhang, L.; Pei, L.; Xue, H.; Li, Z. Adsorption of Methylene Blue and Congo Red from Aqueous Solution on 3D MXene/Carbon Foam Hybrid Aerogels: A Study by Experimental and Statistical Physics Modeling. *J. Environ. Chem. Eng.* **2023**, *11*, 109206. [[CrossRef](#)]
25. Wang, X.; Zhang, A.; Chen, M.; Seliem, M.K.; Mobarak, M.; Diao, Z.; Li, Z. Adsorption of Azo Dyes and Naproxen by Few-Layer MXene Immobilized with Dialdehyde Starch Nanoparticles: Adsorption Properties and Statistical Physics Modeling. *Chem. Eng. J.* **2023**, *473*, 145385. [[CrossRef](#)]
26. Bilici Baskan, M.; Pala, A. Removal of Arsenic from Drinking Water Using Modified Natural Zeolite. *Desalination* **2011**, *281*, 396–403. [[CrossRef](#)]
27. Losev, V.N.; Didukh-Shadrina, S.L.; Orobyeva, A.S.; Metelitsa, S.I.; Borodina, E.V.; Ondar, U.V.; Nesterenko, P.N.; Maznyak, N.V. A New Method for Highly Efficient Separation and Determination of Arsenic Species in Natural Water Using Silica Modified with Polyamines. *Anal. Chim. Acta* **2021**, *1178*, 338824. [[CrossRef](#)]
28. Jacobson, A.T.; Fan, M. Evaluation of Natural Goethite on the Removal of Arsenate and Selenite from Water. *J. Environ. Sci.* **2019**, *76*, 133–141. [[CrossRef](#)] [[PubMed](#)]
29. Ma, M.; Ha, Z.; Lv, C.; Xu, X.; Li, C.; Du, D.; Zhang, T.C.; Chi, R. A Novel Passivator Based on Electrolytic Manganese Residues and Calcite for Arsenic Sorption and Heavy Metal Passivation of Contaminated Soil. *J. Clean. Prod.* **2023**, *414*, 137544. [[CrossRef](#)]
30. Wang, Y.; Liu, H.; Wang, S.; Li, X.; Wang, X.; Jia, Y. Simultaneous Removal and Oxidation of Arsenic from Water by δ -MnO₂ Modified Activated Carbon. *J. Environ. Sci.* **2020**, *94*, 147–160. [[CrossRef](#)]
31. Yao, S.; Liu, Z.; Shi, Z. Arsenic Removal from Aqueous Solutions by Adsorption onto Iron Oxide/Activated Carbon Magnetic Composite. *J. Environ. Health Sci. Eng.* **2014**, *12*, 6–13. [[CrossRef](#)] [[PubMed](#)]
32. Mondal, M.K.; Garg, R. A Comprehensive Review on Removal of Arsenic Using Activated Carbon Prepared from Easily Available Waste Materials. *Environ. Sci. Pollut. Res.* **2017**, *24*, 13295–13306. [[CrossRef](#)] [[PubMed](#)]
33. Shakoor, M.B.; Niazi, N.K.; Bibi, I.; Murtaza, G.; Kunhikrishnan, A.; Seshadri, B.; Shahid, M.; Ali, S.; Bolan, N.S.; Ok, Y.S.; et al. Remediation of Arsenic-Contaminated Water Using Agricultural Wastes as Biosorbents. *Crit. Rev. Environ. Sci. Technol.* **2016**, *46*, 467–499. [[CrossRef](#)]
34. Nagra, M.A.; Natasha, N.; Bibi, I.; Tariq, T.Z.; Naz, R.; Ansar, S.; Shahid, M.; Murtaza, B.; Imran, M.; Khalid, M.S.; et al. Biowaste-Based Sorbents for Arsenic Removal from Aqueous Medium and Risk Assessment. *Environ. Geochem. Health* **2022**. [[CrossRef](#)] [[PubMed](#)]
35. Chatzimichailidou, S.; Xanthopoulou, M.; Tolkou, A.K.; Katsoyiannis, I.A. Biochar Derived from Rice By-Products for Arsenic and Chromium Removal by Adsorption: A Review. *J. Compos. Sci.* **2023**, *7*, 59. [[CrossRef](#)]
36. Tolkou, A.K.; Rada, E.C.; Torretta, V.; Xanthopoulou, M.; Kyzas, G.Z.; Katsoyiannis, I.A. Removal of Arsenic(III) from Water with a Combination of Graphene Oxide (GO) and Granular Ferric Hydroxide (GFH) at the Optimum Molecular Ratio. *C* **2023**, *9*, 10. [[CrossRef](#)]
37. Xanthopoulou, M.; Katsoyiannis, I.A. Enhanced Adsorption of Chromate and Arsenate Ions from Contaminated Water with Emphasis on Polyethylenimine Modified Materials: A Review. *Separations* **2023**, *10*, 441. [[CrossRef](#)]
38. Samimi, M.; Zakeri, M.; Alobaid, F.; Aghel, B. A Brief Review of Recent Results in Arsenic Adsorption Process from Aquatic Environments by Metal-Organic Frameworks: Classification Based on Kinetics, Isotherms and Thermodynamics Behaviors. *Nanomaterials* **2023**, *13*, 60. [[CrossRef](#)]
39. Xu, W.; Wang, J.; Wang, L.; Sheng, G.; Liu, J.; Yu, H.; Huang, X.J. Enhanced Arsenic Removal from Water by Hierarchically Porous CeO₂-ZrO₂ Nanospheres: Role of Surface- and Structure-Dependent Properties. *J. Hazard. Mater.* **2013**, *260*, 498–507. [[CrossRef](#)]

40. Tolkou, A.K.; Kyzas, G.Z.; Katsoyiannis, I.A. Arsenic(III) and Arsenic(V) Removal from Water Sources by Molecularly Imprinted Polymers (MIPs): A Mini Review of Recent Developments. *Sustainability* **2022**, *14*, 5222. [[CrossRef](#)]
41. Koutzaris, S.; Xanthopoulou, M.; Laskaridis, A.; Katsoyiannis, I.A. H₂O₂-Enhanced As(III) Removal from Natural Waters by Fe(III) Coagulation at Neutral PH Values and Comparison with the Conventional Fe(II)-H₂O₂ Fenton Process. *Sustainability* **2022**, *14*, 6306. [[CrossRef](#)]
42. Zheng, Q.; Hou, J.; Hartley, W.; Ren, L.; Wang, M.; Tu, S.; Tan, W. As(III) Adsorption on Fe-Mn Binary Oxides: Are Fe and Mn Oxides Synergistic or Antagonistic for Arsenic Removal? *Chem. Eng. J.* **2020**, *389*, 124470. [[CrossRef](#)]
43. Tolkou, A.K.; Trikalioti, S.; Makrogianni, O.; Xanthopoulou, M.; Deliyanni, E.A.; Kyzas, G.Z.; Katsoyiannis, I.A. Lanthanum Modified Activated Carbon from Coconut Shells for Chromium (VI) Removal from Water. *Nanomaterials* **2022**, *12*, 1067. [[CrossRef](#)] [[PubMed](#)]
44. Tolkou, A.K.; Trikalioti, S.; Makrogianni, O.; Katsoyiannis, I.A.; Kyzas, G.Z. Magnesium Modified Activated Carbons Derived from Coconut Shells for the Removal of Fluoride from Water. *Sustain. Chem. Pharm.* **2023**, *31*, 100898. [[CrossRef](#)]
45. Sujiono, E.H.; Zabrian, D.; Zharvan, V.; Humairah, N.A. Fabrication and Characterization of Coconut Shell Activated Carbon Using Variation Chemical Activation for Wastewater Treatment Application. *Results Chem.* **2022**, *4*, 100291. [[CrossRef](#)]
46. Kyzas, G.Z.; Deliyanni, E.A. Modified Activated Carbons from Potato Peels as Green Environmental-Friendly Adsorbents for the Treatment of Pharmaceutical Effluents. *Chem. Eng. Res. Des.* **2015**, *97*, 135–144. [[CrossRef](#)]
47. Heidarinejad, Z.; Dehghani, M.H.; Heidari, M.; Javedan, G.; Ali, I.; Sillanpää, M. Methods for Preparation and Activation of Activated Carbon: A Review. *Environ. Chem. Lett.* **2020**, *18*, 393–415. [[CrossRef](#)]
48. Sultana, M.; Rownok, M.H.; Sabrin, M.; Rahaman, M.H.; Alam, S.M.N. A Review on Experimental Chemically Modified Activated Carbon to Enhance Dye and Heavy Metals Adsorption. *Clean. Eng. Technol.* **2022**, *6*, 100382. [[CrossRef](#)]
49. Wang, Y.; Liu, Y.; Guo, T.; Liu, H.; Li, J.; Wang, S.; Li, X.; Wang, X.; Jia, Y. Lanthanum Hydroxide: A Highly Efficient and Selective Adsorbent for Arsenate Removal from Aqueous Solution. *Environ. Sci. Pollut. Res.* **2020**, *27*, 42868–42880. [[CrossRef](#)] [[PubMed](#)]
50. Sawana, R.; Somasundar, Y.; Iyer, V.S.; Baruwati, B. Ceria Modified Activated Carbon: An Efficient Arsenic Removal Adsorbent for Drinking Water Purification. *Appl. Water Sci.* **2017**, *7*, 1223–1230. [[CrossRef](#)]
51. Merodio-Morales, E.E.; Reynel-Ávila, H.E.; Mendoza-Castillo, D.I.; Duran-Valle, C.J.; Bonilla-Petriciolet, A. Lanthanum- and Cerium-Based Functionalization of Chars and Activated Carbons for the Adsorption of Fluoride and Arsenic Ions. *Int. J. Environ. Sci. Technol.* **2020**, *17*, 115–128. [[CrossRef](#)]
52. Yanagisawa, H.; Matsumoto, Y.; Machida, M. Adsorption of Zn(II) and Cd(II) Ions onto Magnesium and Activated Carbon Composite in Aqueous Solution. *Appl. Surf. Sci.* **2010**, *256*, 1619–1623. [[CrossRef](#)]
53. Choong, C.E.; Ibrahim, S.; Yoon, Y.; Jang, M. Removal of Lead and Bisphenol A Using Magnesium Silicate Impregnated Palm-Shell Waste Powdered Activated Carbon: Comparative Studies on Single and Binary Pollutant Adsorption. *Ecotoxicol. Environ. Saf.* **2018**, *148*, 142–151. [[CrossRef](#)]
54. Irunde, R.; Ligate, F.J.; Ijumulana, J.; Ahmad, A.; Maity, J.P.; Hamisi, R.; Philip, J.Y.N.; Kilulya, K.F.; Karlton, E.; Mtamba, J.; et al. The Natural Magnesite Efficacy on Arsenic Extraction from Water and Alkaline Influence on Metal Release in Water. *Appl. Geochem.* **2023**, *155*, 105705. [[CrossRef](#)]
55. Sugita, H.; Oguma, T.; Hara, J.; Zhang, M.; Kawabe, Y. Removal of Arsenate from Contaminated Water via Combined Addition of Magnesium-Based and Calcium-Based Adsorbents. *Sustainability* **2023**, *15*, 4689. [[CrossRef](#)]
56. Swenson, H.; Stadie, N.P. Langmuir's Theory of Adsorption: A Centennial Review. *Langmuir* **2019**, *35*, 5409–5426. [[CrossRef](#)]
57. Freundlich, H. Über Die Adsorption in Lösungen. *Z. Phys. Chem.* **1907**, *57U*, 385–470. [[CrossRef](#)]
58. Smith, A.H.; Steinmaus, C.M. Health Effects of Arsenic and Chromium in Drinking Water: Recent Human Findings. *Annu. Rev. Public Health* **2009**, *30*, 107–122. [[CrossRef](#)]
59. Sotomayor, F.; Quantatec, A.P.; Sotomayor, F.J.; Cychosz, K.A.; Thommes, M. Characterization of Micro/Mesoporous Materials by Physisorption: Concepts and Case Studies. *Acc. Mater. Surf. Res.* **2018**, *3*, 34–50.
60. Nasri, N.S.; Jibril, M.; Zaini, M.A.A.; Mohsin, R.; Dadum, H.U.; Musa, A.M. Synthesis and Characterization of Bio-Based Porous Carbons by Two Step Physical Activation with CO₂. *J. Teknol.* **2014**, *68*, 5–9. [[CrossRef](#)]
61. Jais, F.M.; Ibrahim, S.; Yoon, Y.; Jang, M. Enhanced Arsenate Removal by Lanthanum and Nano-Magnetite Composite Incorporated Palm Shell Waste-Based Activated Carbon. *Sep. Purif. Technol.* **2016**, *169*, 93–102. [[CrossRef](#)]
62. Dudek, S.; Kołodziejka, D. Arsenic(V) Removal on the Lanthanum-Modified Ion Exchanger with Quaternary Ammonium Groups Based on Iron Oxide. *J. Mol. Liq.* **2022**, *347*, 117985. [[CrossRef](#)]
63. Mehanathan, S.; Jaafar, J.; Nasir, A.M.; Ismail, A.F.; Matsuura, T.; Othman, M.H.D.; Rahman, M.A.; Yusof, N. Magnesium Oxide Nanoparticles for the Adsorption of Pentavalent Arsenic from Water: Effects of Calcination. *Membranes* **2023**, *13*, 475. [[CrossRef](#)]
64. Mudzielwana, R.; Gitari, M.W. Removal of Fluoride from Groundwater Using MnO₂ Bentonite-Smectite Rich Clay Soils Composite. *Groundw. Sustain. Dev.* **2021**, *14*, 100623. [[CrossRef](#)]
65. Tolkou, A.K.; Trikaliotis, D.G.; Kyzas, G.Z.; Katsoyiannis, I.A.; Deliyanni, E.A. Simultaneous Removal of As(III) and Fluoride Ions from Water Using Manganese Oxide Supported on Graphene Nanostructures (GO-MnO₂). *Sustainability* **2023**, *15*, 1179. [[CrossRef](#)]
66. Katsoyiannis, I.A.; Voegelin, A.; Zouboulis, A.I.; Hug, S.J. Enhanced As(III) Oxidation and Removal by Combined Use of Zero Valent Iron and Hydrogen Peroxide in Aerated Waters at Neutral PH Values. *J. Hazard. Mater.* **2015**, *297*, 1–7. [[CrossRef](#)] [[PubMed](#)]

67. Banerjee, K.; Nour, S.; Selbie, M.; Prevost, M.; Blumenschein, C.D.; Chen, H.; Amy, G.L. *Optimization of Process Parameters for Arsenic Treatment with Granular Ferric Hydroxide*; American Water Works Association: Denver, CO, USA, 2003.
68. Banerjee, S.; Chattopadhyaya, M.C. Adsorption Characteristics for the Removal of a Toxic Dye, Tartrazine from Aqueous Solutions by a Low Cost Agricultural by-Product. *Arab. J. Chem.* **2017**, *10*, S1629–S1638. [[CrossRef](#)]
69. Pourhakkak, P.; Taghizadeh, A.; Taghizadeh, M.; Ghaedi, M.; Haghdoost, S. Fundamentals of Adsorption Technology. *Interface Sci. Technol.* **2021**, *33*, 1–70. [[CrossRef](#)]
70. Yin, Y.; Zhou, T.; Luo, H.; Geng, J.; Yu, W.; Jiang, Z. Adsorption of Arsenic by Activated Charcoal Coated Zirconium-Manganese Nanocomposite: Performance and Mechanism. *Colloids Surf. A Physicochem. Eng. Asp.* **2019**, *575*, 318–328. [[CrossRef](#)]
71. Kyzas, G.Z.; Christodoulou, E.; Bikiaris, D.N. Basic Dye Removal with Sorption onto Low-Cost Natural Textile Fibers. *Processes* **2018**, *6*, 166. [[CrossRef](#)]
72. Chen, W.; Luan, J.; Yu, X.; Wang, X.; Ke, X. Preparation of Core-Shell Structured Polystyrene @ Graphene Oxide Composite Microspheres with High Adsorption Capacity and Its Removal of Dye Contaminants. *Environ. Technol.* **2021**, *42*, 3840–3851. [[CrossRef](#)]
73. Sahu, N.; Singh, J.; Koduru, J.R. Removal of Arsenic from Aqueous Solution by Novel Iron and Iron–Zirconium Modified Activated Carbon Derived from Chemical Carbonization of Tectona Grandis Sawdust: Isotherm, Kinetic, Thermodynamic and Breakthrough Curve Modelling. *Environ. Res.* **2021**, *200*, 111431. [[CrossRef](#)]
74. Koohzad, E.; Jafari, D.; Esmaili, H. Adsorption of Lead and Arsenic Ions from Aqueous Solution by Activated Carbon Prepared from Tamarix Leaves. *ChemistrySelect* **2019**, *4*, 12356–12367. [[CrossRef](#)]
75. Esmaili, H.; Mousavi, S.M.; Hashemi, S.A.; Chiang, W.H.; Ahmadpour Abnavi, S. Activated Carbon@MgO@Fe₃O₄ as an Efficient Adsorbent for As (III) Removal. *Carbon Lett.* **2021**, *31*, 851–862. [[CrossRef](#)]
76. Prajapati, A.K.; Mondal, M.K. Hazardous As(III) Removal Using Nanoporous Activated Carbon of Waste Garlic Stem as Adsorbent: Kinetic and Mass Transfer Mechanisms. *Korean J. Chem. Eng.* **2019**, *36*, 1900–1914. [[CrossRef](#)]
77. Shi, J.; Zhao, Z.; Zhou, J.; Sun, T.; Liang, Z. Enhanced Adsorption of As(III) on Chemically Modified Activated Carbon Fibers. *Appl. Water Sci.* **2019**, *9*, 41. [[CrossRef](#)]
78. Chuc, P.N.; Bac, N.Q.; Thao, D.T.P.; Kien, N.T.; Chi, N.T.H.; Noi, N.V.; Nguyen, V.T.; Bich, N.T.H.; Nhiem, D.N.; Khieu, D.Q. Highly Efficient Adsorption of Arsenite from Aqueous by Zirconia Modified Activated Carbon. *Environ. Eng. Res.* **2024**, *29*, 230070–230076. [[CrossRef](#)]

Disclaimer/Publisher’s Note: The statements, opinions and data contained in all publications are solely those of the individual author(s) and contributor(s) and not of MDPI and/or the editor(s). MDPI and/or the editor(s) disclaim responsibility for any injury to people or property resulting from any ideas, methods, instructions or products referred to in the content.